An Optimizer Using the PSO Algorithm to Determine Thermal Parameters of PCM: A case study of grey water heat harnessing

Mazhar AR, Liu S, Shukla A.

DOI 10.1016/j.ijheatmasstransfer.2019.118574
ISSN 0017-9310
Publisher: Elsevier

An Optimizer Using the PSO Algorithm to Determine Thermal Parameters of PCM: A case study of grey water heat harnessing

Abdur Rehman Mazhar, Shuli Liu[1], Ashish Shukla

School of Energy, Construction and Environment, Coventry University, Coventry, CV1 2HF, United Kingdom

Abstract

The melting and freezing of Phase Change Materials (PCMs) is categorized as a moving boundary problem. For this reason the mathematical solution to study the behaviour of practical applications is only possible via complex numerical approximations. However for a preliminary design the main concern is to select the optimum thermal characteristics of the PCM storage unit, for both melting and freezing. This is to be done before the detailed design by integrating an optimization algorithm with a numerical simulation. The application of using PCMs to harness the waste heat from non-industrial grey water is investigated as a case of study. For this purpose, the 2-phase analytical solution to the Stefan problem is coupled with the particle swarm optimizer (PSO) to find the best combination of thermal characteristics within the prescribed boundary conditions of this case study. Results show that the optimum phase change temperature lies between 20-22°C, depending on various sets of input parameters. At the same time the ratio of latent to sensible heat transferred by the PCM highly influences this optimum temperature for the combination of both melting and freezing. Similarly results show melting being faster and more intensive in term of latent heat charging compared to a higher sensible heat discharging while freezing.

Keywords: Stefan problem, Particle swarm optimization, Neumann solution, Thermal characteristics, Phase change materials

[1]Corresponding author Tel: +44 (0) 24 7765 7822; Fax.: +44 (0) 2477658296
Email: aa6328@coventry.ac.uk

1. Introduction

Harnessing waste heat from grey water (GW) in non-industrial buildings, has been highlighted to reduce the carbon footprint of passive houses [1]. Currently conventional heat pumps and exchangers are the only viable commercial options for this application. However to decouple demand with supply and integrate high density thermal storage in these heat extracting devices, the use of phase change materials (PCMs) is proposed. In the simplest design, a conventional hot GW pipe in a building is coupled to a mains cold water (CW) pipe linked with a PCM in an enclosed container, as in Figure 1.

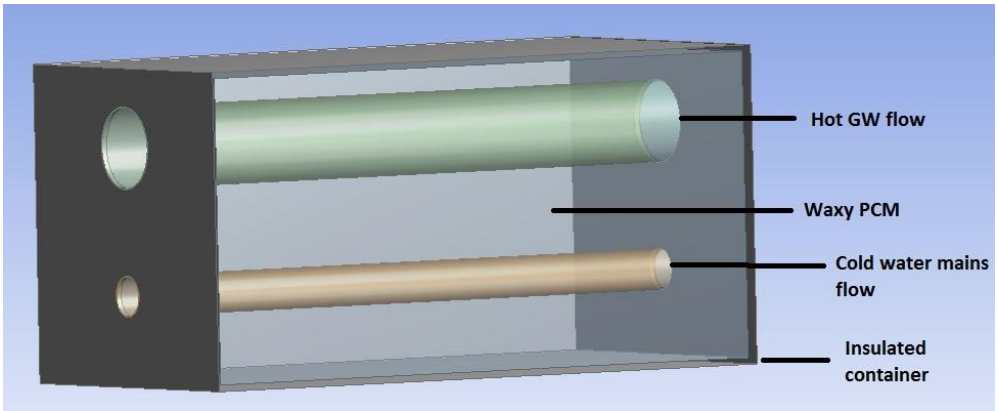

Figure 1: Simplest GW heat harnessing exchanger with PCM as thermal storage

In this configuration, the incoming GW is at about 40-70°C, losing its heat to the surrounding PCM. The PCM melts and upon an incoming flow of CW at about 5-15°C, it freezes back to give away the stored heat. Several thermal improvements can be made to the simple design of Figure 1, including enhancing the thermal conductivity of the PCM, but is out of the scope of this paper.

For the selection of the thermal parameters of the PCM for this application, the 2-phase analytical solution of the Stefan problem (Neumann solution) is best suited for this optimization analysis. In this method the net heat flux of melting and freezing is calculated with reference to the specific phase change temperature which must be optimized. At the

same time the Particle Swarm Optimizer (PSO) optimizer has minimal requirements and guarantees fast convergence of an array of variables within specified limits [2]. This is a class of immensely famous optimizers mimicking social behaviour using artificial intelligence techniques.

With the demand of high density thermal storage with isothermal conditions, PCMs have been in the limelight over the past few years. Several theoretical studies have been conducted for the assessment of an idea and to carry out a basic system design [3–6]. At the same time, to study the effects of a PCM used in conjunction with other systems, several studies on simulation platforms have been conducted [7,8]. To carry out these basic designs and ideas forward, there have been many feasibility studies of evaluating PCMs in specific applications [9–12]. The performance of these design parameters usually in terms of dimensional aspects, have been the focus of many optimization algorithms [13–17]. Similarly most of these studies have been done in laboratory conditions or in experiment to evaluate the PCMs practically [18–21]. Several numerical solutions have been the main focus of research. Many variants of the two main numerical methods: the enthalpy and the effective heat capacity method have been abundantly used with minor modifications. Most simulations are 2-D due to limitations in computing power and economic constraints, on common commercially available software's including ANSYS, Star-CCM, Comsol, OpenFoam, MATLAB etc. [22–24]. However usually both numerical and experimental studies are carried out in conjunction with each other, especially for validation purposes [25,26]. Finally the mathematics and thermodynamics of melting and freezing are different from each other. Several studies emphasize on melting [27] while others focus only on freezing [28] of PCMs. Only a handful, focus on both these aspects, together [29,30].

Most literature has been based on initial feasibility studies or a detailed design analysis with regards to specific applications. They do not describe a strategy to select a PCM in the initial phases of design based on predefined boundary conditions especially with regards to the GW application. Most published PCM applications are limited to the cooling of batteries/electronics, solar thermal heating, passive heating/cooling technologies with air, usage in building walls, waste heat harnessing in automotive applications and enhancing the storage efficiency in existing thermal storages. In terms of optimization strategies, they have mostly been done without a specific technique by simply testing discrete variants of a design either experimentally or numerically. At the same time, most literature either focus on the numerical solving of the Stefan problem or experimentally analysing the effects of PCMs. Only partial behaviour is considered with modelling either melting or freezing, depending on the emphasis of the application. For a preliminary design, the selection of a PCM based on both freezing and melting using an analytical solution with an evolutionary optimizer is not to be found in literature. The main aim of this paper is to define the methodology to select the optimum thermal characteristics of the PCM to maximize both the heat extracted from the GW and the heat released back to the CW, based on the GW design presented in Figure 1. This could not be done using sophisticated numerical techniques of mainstream Computational Fluid Dynamics (CFD) software's as it requires a basic optimization algorithm to be integrated as well, based on a range of thermal parameters of the PCM. The following objectives will be carried out:

- Formulate a 2-phase analytical solution based on the thermal parameters of the PCM, for both melting and freezing;
- Integrate the PSO algorithm with this solution based on the prescribed boundary conditions of the GW heat harnessing application;

- Optimize the thermal parameters for both the solution and the optimizer, with the aim of maximizing the net heat flux; and
- Perform a sensitivity analysis of the main parameters affecting the outcome of the solution.

2. Physical concept and mathematical models

2.1. Stefan problem and the Neumann solution

2.1.1. Physical concept of the Stefan problem

The most common phase change phenomena used in engineering applications is the solid-liquid type [32] and the Stefan problem mathematically defines the melting and freezing of it. It is non-linear and the greatest difficulty lies in the fact that unknown variables exist in a region which is yet to be solved e.g. the to-be liquid region in the melting of an initial solid. Due to the dependency on the phase change front and its variation with time, the Stefan problem is mathematically categorized as a ‘moving boundary problem’. Depending on the simplifications and accuracy required, many variant methods for the solution are summarized in

Figure 2**Error! Reference source not found.**:

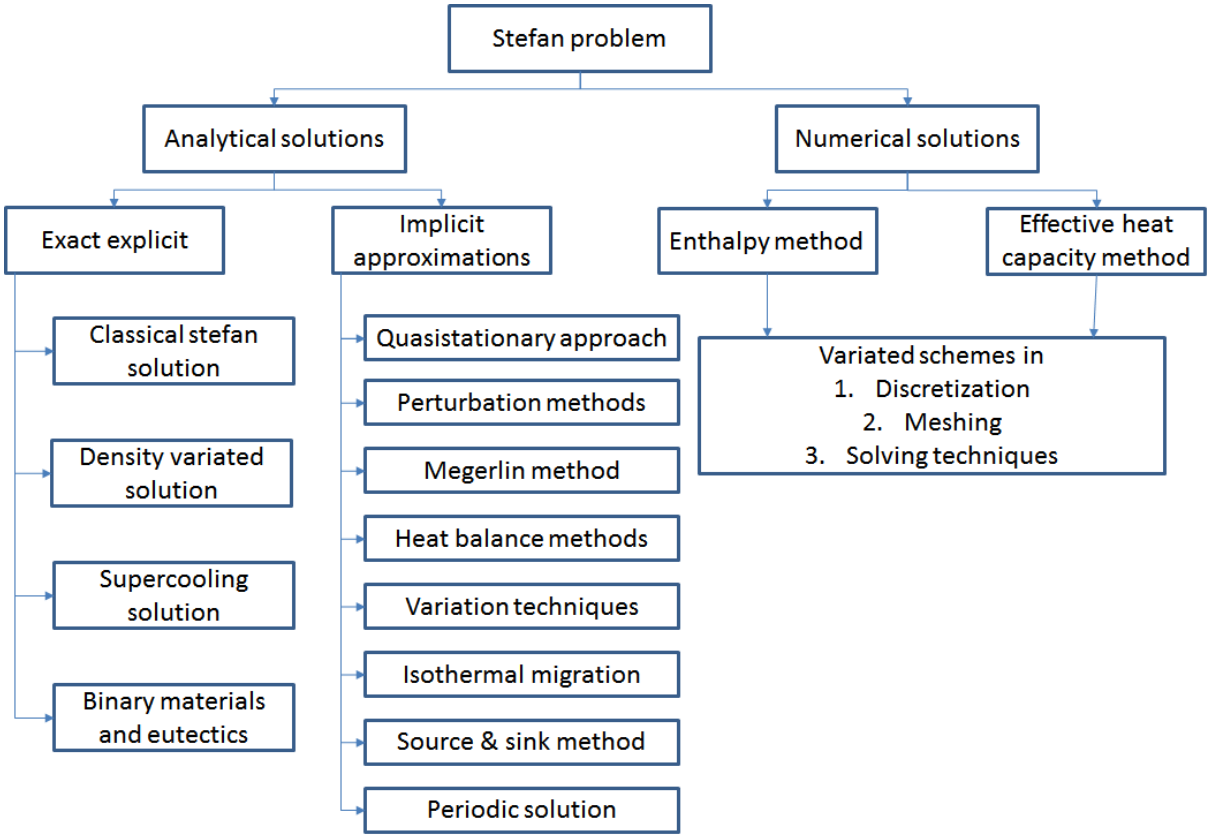

Figure 2: Solution methods to the Stefan problem

The exact explicit solutions are known as the classical or Neumann solutions, but involve many simplifications and are 1-D. They are the basis of understanding the different thermal parameters involved and a good approximation to real scenarios [31]. Many 3-D applications can be accurately simplified, using this classical 1-D approach [38]. Implicit approximations are also based on various simplifications and assumptions, but reasonably model more practical configurations [32]. They are generally used as an initial estimate of a real setup after validation through experimentation or a numerical analysis, as in many studies [33,34]. Numerical solutions are more accurate, at the cost of more computation time and resources. There exist many variants to this method and is a wide field in CFD [35–37].

In this study the exact explicit 2-Phase analytical solution to the Stefan problem is used, with the following assumptions [35]:

1) The PCM has constant thermal parameters for both phases. Usually a material has an abrupt change after phase transition in only its density by about 5 – 30% [38], causing discontinuities in the solution. All parameters have no discontinuity and are smooth functions of temperature.
2) Heat transfer is isotropic only by conduction. Heat flow is normal to the surface and is unidirectional;
3) The phase change interface is sharp, planar, has zero-thickness and occurs only at the isothermal temperature 'T_m'. There is only one phase change front, and multiple cycles have no impact over the thermal properties;
4) No internal heat source or sink is present within the PCM. There is no decrease in the temperature of a point within the domain, and is always rising or constant, for melting. Vice versa for freezing and;
5) Nucleation, supercooling, surface effects, curvature effects are neglected.

The heat equation expresses the conservation of heat locally predicting the temperature distribution in terms of position and time, being applicable in the solid and liquid PCM regions, separated by the interface as:

$$\frac{\partial T}{\partial t} = \alpha \nabla^2 T + \dot{q} \tag{1}$$

As in Figure 3, for the Neumann solution a 1-D semi-infinite slab is initially at a temperature 'T_i', with the application of a constant temperature 'T_b' at the left-hand boundary at time

't=0'. The discontinuity at this initial time 't_0' from 'T_i' to 'T_b', implies that the temperature changes at an infinite rate. Although this may seem, unreasonable but for theoretical calculations in a semi-infinite domain with relatively small temperature gradients, the equation is applicable.

Before a solid can melt it must acquire a specific amount of energy to overcome the bonding forces within it or similarly a liquid must exothermically release this energy to transit to a solid, at a phase change temperature 'T_m'. This energy is called the latent heat 'L', representing, the difference in enthalpy levels between both phases at similar conditions, and is known as the Stefan condition at the melt interface. The enthalpy of the liquid phase is higher than the solid phase, the difference of which is the required heat flux across the interface for phase change [39]. This required net heat flux across the interface is equal to the rate of transfer of latent heat per unit area across it. The velocity 'v' of the interface is equal to the rate of change of this net heat flux. The heat flux across the interface is continuous only when 'L = 0' or the interface is stationary. This Stefan condition is defined as:

$$\rho L \dot{X(t)} = -k_L \frac{\partial T}{\partial x}(X(t)^-, t) + k_S \frac{\partial T}{\partial x}(X(t)^+, t) \tag{2}$$

'$X(t)$' is the position of the melt front with the superscripts, donating the side of approach.

A summary of the applicable equations, boundary and initial conditions, for this melting phenomena are in Figure 3, where the solid black lines represent the boundaries and the interface.

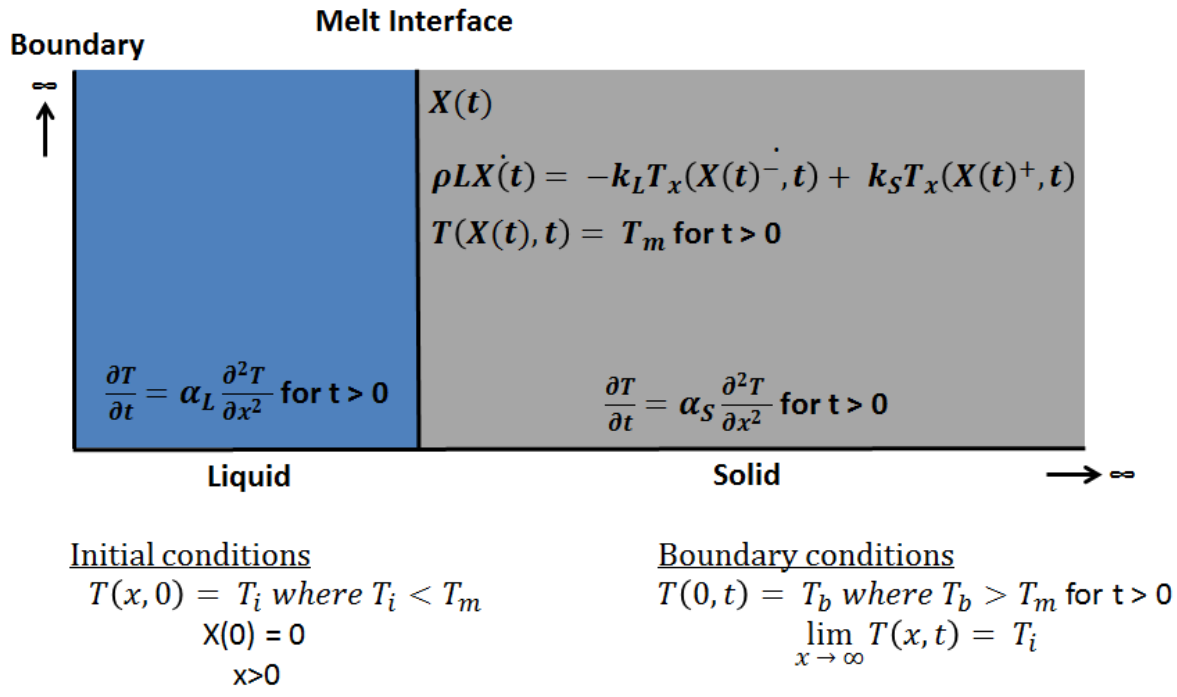

Figure 3: Boundary and initial conditions of the simplified 2-Phase Stefan problem

2.1.2. Mathematical formulation of the 2-phase analytical (Neumann) solution

This Stefan problem for this semi-infinite case with a constant temperature boundary condition is solved via the separation of variables technique [39]. In the solution, three important relationships are of interest:

- The temperature distribution within both phases
- The location and speed of the interface
- The amount of heat stored and released while melting and freezing

The explicit solution of Figure 3 is the classical 2-Phase analytical or the Neumann solution [39]. This 1-D slab case is different from the pipe-container configuration of Figure 1, but is a good approximation of a comparative assessment of melting and freezing. Unless the pipe radius is very small, the freezing or melting around a pipe is roughly slab-like [38]. The slow

heat of conduction and transition in phase of the PCM, makes a reasonable approximation of an infinite slab to a real finite slab.

Three variables defining the outcome of the solution are:

$$St_L = \frac{c_L(T_b - T_m)}{L}, \quad St_S = \frac{c_S(T_m - T_i)}{L}, \qquad a = \sqrt{\frac{\alpha_L}{\alpha_S}} \tag{3}$$

The Stefan numbers (St) represent the ratio of the sensible heat to the latent heat for both phases. For certain waxes or organic PCMs, it is usually small, hence the bulk of the heat transfer is in latent form, as in this application of GW using organic PCMs. For metals it is usually 1 – 10 where sensible heating effects cannot be neglected. Normally for ceramics and silicates it is very large with negligible latent effects [40].

Based on the method of similarity variables, 'λ', is defined as the root to a transcendental equation [32]. For each value of the Stefan numbers there exists a unique solution of 'λ' implying a uniqueness of the Neumann solution [41]. The transcendental equation is:

$$f(\lambda) = \frac{St_L}{\exp(\lambda^2)\,\mathrm{erf}(\lambda)} - \frac{St_S}{(a\,\exp(a^2\lambda^2) erfc(a\lambda)} - \lambda\sqrt{\pi} \tag{4}$$

More accurate solutions to this transcendental equation may be found using Brent's method [41]. This equation is solvable with the Newton-Raphson iterative method, with an initial estimate 'λ_0', defined as:

$$\lambda_0 = 0.5\left[-\frac{St_S}{a\sqrt{\pi}} + \sqrt{2St_L + \left(\frac{St_S}{a\sqrt{\pi}}\right)^2}\right] \tag{5}$$

Based on this solution, the position of the melt front can be computed as:

$$X(t) = 2\lambda\sqrt{\alpha_L t} \qquad t > 0 \tag{6}$$

The temperature in the liquid region is defined as,

$$T(x,t) = T_b - (T_b - T_m)\frac{erf\left[\frac{x}{2\sqrt{\alpha_L t}}\right]}{erf\lambda} \qquad 0 < x < X(t) \text{ and } t > 0 \tag{7}$$

While the temperature in the solid region is,

$$T(x,t) = T_i + (T_m - T_i)\frac{erfc\left[\frac{x}{2\sqrt{\alpha_S t}}\right]}{erfc(\lambda a)} \qquad x > X(t) \text{ and } t > 0 \tag{8}$$

For melting, at any time interval 't > 0' the liquid occupies the region (0, X (t)) while the solid occupies (X (t), ∞).

At 't=0' the system has zero energy at a temperature 'T_i'. Based on this the total heat entering the system for melting, is:

$$Q(t) = \int_0^t q(0,t)dt = \int_0^t -k_L\frac{\partial T}{\partial x}(0,t)dt = \frac{\rho L St_L X(t)}{\sqrt{\pi}\lambda erf\lambda} \tag{9}$$

The total energy absorbed by the system is the sensible heat to the liquid, solid and the latent heat. The sensible heat added to the liquid phase is:

$$Q_L^{sens}(t) = \int_0^{X(t)} \rho\, C_s(T_m - T_i)dx + \int_0^{X(t)} \rho\, C_L(T(x,t) - T_m)dx \qquad (10)$$

$$= \rho L St_S X(t) + \rho L St_L X(t) \frac{1 - e^{-\lambda^2}}{\sqrt{\pi}\lambda erf\lambda}$$

The sensible heat added to the solid phase is:

$$Q_S^{sens}(t) = \int_{X(t)}^{\infty} \rho\, C_s(T(x,t) - T_i)dx \qquad (11)$$

$$= \rho L St_S X(t) \left[\frac{1}{\sqrt{\pi}a\lambda e^{(a\lambda)^2} erfc(a\lambda)} - 1\right]$$

The latent heat added to the system is:

$$Q^{lat}(t) = \rho L X(t) \qquad (12)$$

To verify that the energy balance is satisfied the following holds:

$$Q_L^{sens} + Q_S^{sens} + Q^{lat} = Q \qquad (13)$$

Heat conduction in a semi-infinite slab for the case of the freezing process where '$T_i > T_m$' and '$T_b < T_m$' is also modelled [38]. The changed variables and equations are defined as follows, with all other parameters remaining the same:

The Stefan numbers are

$$St_L = \frac{c_L(T_i - T_m)}{L}, \quad St_S = \frac{c_S(T_m - T_b)}{L} \tag{14}$$

The transcendental equation is now defined as:

$$f(\lambda) = \frac{St_S}{\exp(\lambda^2)\,\mathrm{erf}(\lambda)} - \frac{St_L}{(a\exp(a^2\lambda^2)erfc(a\lambda)} - \lambda\sqrt{\pi} \tag{15}$$

The initial estimate to the root 'λ', for the Newton-Raphson method is as follows:

$$\lambda_0 = 0.5\left[-\frac{St_L}{a\sqrt{\pi}} + \sqrt{2St_S + \left(\frac{St_L}{a\sqrt{\pi}}\right)^2}\right] \tag{16}$$

The position of the freezing front is defined as:

$$X(t) = 2\lambda\sqrt{\alpha_S t} \qquad t > 0 \tag{17}$$

The temperature in the liquid region is:

$$T(x,t) = T_i + (T_m - T_i)\frac{erfc\left[\frac{x}{2\sqrt{\alpha_L t}}\right]}{erfc(\lambda a)} \qquad \mathrm{x} > \mathrm{X(t)\ and\ t} > 0 \tag{18}$$

While the temperature in the solid region is:

$$T(x,t) = T_b - (T_b - T_m)\frac{erf\left[\frac{x}{2\sqrt{\alpha_L t}}\right]}{erf\lambda} \qquad 0 < x < X(t) \text{ and } t > 0 \tag{19}$$

In the event that '$T_i < T_m$', the case of conduction in the liquid slab is witnessed, as will be seen as a possibility in section 3. For this the temperature profile in the un-frozen liquid PCM is:

$$T(x,t) = T_b - (T_b - T_i)erf\left(\frac{x}{2\sqrt{\alpha_S t}}\right) \tag{20}$$

The total heat input to the system is defined as:

$$Q(t) = \frac{\rho L S t_S X(t)}{\sqrt{\pi}\lambda erf\lambda} \tag{21}$$

The sensible heat addition to the liquid phase is:

$$Q_L^{sens}(t) = \rho L S t_L X(t) + \rho L S t_S X(t)\frac{1 - e^{-\lambda^2}}{\sqrt{\pi}\lambda erf\lambda} \tag{22}$$

While that to the solid phase is:

$$Q_S^{sens}(t) = \rho L S t_L X(t)\left[\frac{1}{\sqrt{\pi}a\lambda e^{(a\lambda)^2} erfc(a\lambda)} - 1\right] \tag{23}$$

2.2. Particle swarm optimizer

2.2.1. Physical concept of the PSO

The optimization of the Stefan problem for melting and freezing in GW is multi-dimensional and non-linear requiring a not so computational intensive zero-order simple optimizer. Zero-order methods use only values of the objective function without using their derivatives [42]. Zero-order bracketing methods have higher computation times with chances of converging to local optimums instead of global ones. On the other hand, zero-order evolutionary methods are used to solve non-linear, non-convex and even discontinuous applications at a reasonable speed with simple algorithms, being more applicable in this scenario.

Although there are about 40 different nature inspired, artificial intelligence evolutionary methods the three most famous techniques are analysed in Table 1 [43] [44].

Table 1: Advantages and disadvantages of the main evolutionary methods

	Advantages	**Disadvantages**
Particle swarm method	• Applicable in a range of problems (robust) • Simplest of all with fewest variables • Fastest convergence • Adapts to multi dimensions without any side affect • Insensitive to scaling of design variables • Oldest method with several custom modifications possible	• Chances of local optima are highly possible • Not applicable for noisy problems • Requires a multi-dimensional coordinate system • Parameters for each problem require custom tuning
Ant colony method	• Applicable in dynamic problems • Inherent parallelism • Large parameter ranges possible • Closest replication to real social behavior • Manages external affects more efficiently	• Theoretically difficult algorithm • Comparatively a high number of variables • Probabilities and chance factors must be computed for each iteration • Convergence time uncertain and highly dependent on initial estimate

Firefly algorithm	• Applicable for noisy multi-peak problems • Latest and newest of the evolutionary methods • Hybrid combinations easily possible • Applicable to discontinuous functions	• Comparatively slow convergence rates • Probability of the local optima trap is the greatest • A high number of variables and complexity • Custom modification of the entire algorithm as per problem is required • Extra behavioral information of the problem is required

Based on these considerations and experimental research, the PSO method is deemed the most feasible for this Neumann-GW application [45]. The fact that the PSO optimizer should search through multidimensional space arrays, without taking the derivative of the function, even if it is noisy, discontinuous or irregular make it suitable. However, an important drawback is that sometimes, if the parameters are not properly tuned, it may lead to premature convergence to the local optimum.

PSO is based on the collective behaviour of multiple interacting particles (birds). Each particle can be considered as unintelligent, but the collective system of the swarm is intelligent as it shows self-organization behaviour. The self-organization, co-evolution and learning of these particles, after each iteration, ensure its convergence to the optimized point. It is categorized as a generic population-based metaheuristic optimization algorithm [46]. Several hybrid and modified versions have evolved with an increasing popularity in the field of optimization, but the most basic is used in conjunction with the Neumann solution.

2.2.2. Mathematical formulation of the PSO

In the PSO algorithm, particles evolve by communicating with their neighbours and by learning from their mistakes. Only the position and velocity of each particle in the swarm

changes, as the entire swarm heads towards the optimum solution [47]. The following steps constitute the PSO algorithm, used in this application [45] [48]:

- The set of variables to be optimized and the output value (fitness) determining the optimum is identified.
- The number of iterations, and associated parameters of the PSO algorithm are defined.
- The search space for each variable is defined, in a range between a maximum and minimum. Each variable is a dimension of the PSO represented by an element in the position vector of a particle.
- The PSO is initialized with a fixed sized population (particles) of random solutions. The rule of thumb is that the number of particles should be up to four times the number of optimizable variables (dimensions). The position of any particle, in an iteration, in the search space is a vector of 'n' dimensions representing each optimizable variable, used to find the fitness function or the potential solution. As an example, the position of a particle in iteration 'k' is represented with 'n' variables '*x*' as $x_i(k) = (x_1, x_2 \ldots\ldots x_n)$.
- Each particle has a velocity which governs its position in the coming iteration. The velocity is a vector, like the position vector that guides the particle to move to a potentially better position. The position and velocity of each particle is updated after each iteration. The velocity of a particle is also represented by 'n' variables '*v*', $v_i(k) = (v_1, v_2 \ldots\ldots v_n)$. In the first iteration the velocity vector is randomized like the position vector.
- The fitness '$f(x)$', for each particle is computed, based on the optimizable output function defined in the first step.

- A given particle's position in the next iteration is influenced by its own learning represented by the variable 'pBest', also an 'n' dimension vector, $pBest_i(k) = (pBest_1, pBest_2 \ldots\ldots pBest_n)$. The best personal position discovered by the particle is updated after each iteration, as defined by the fitness value in the last step. If in a specified iteration 'k' the position of the particle is better than its previous best, it is updated, for each dimension, otherwise it is kept same. In the first iteration 'pBest' for each particle is initialized to the first position. For a given iteration each dimension in 'pBest', is updated according to the simple logic:

$$pBest_i(k+1) = \begin{cases} pBest_i(k) & if \quad f(x_i(k)) \leq f(pBest_i(k)) \\ x_i(k) & if \quad f(x_i(k)) > f(pBest_i(k)) \end{cases} \tag{24}$$

  A greater than sign for the fitness assumes a better condition, although the logic can vary in case a minima is the optimal solution. In this case a maxima is desired, as explained in section 3.

- A given particles position in the next iteration is also influenced by the best position of the entire swarm or its social network. It is represented by the variable 'sBest', also an 'n' dimension vector, $\text{sBest}(k) = (sBest_1, sBest_2 \ldots\ldots sBest_n)$. The best personal position discovered by the swarm is updated after each iteration, as defined by the fitness value. To find the best position of the entire swarm 'sBest' is compared to the 'pBest' of each particle in an iteration, as:

$$sBest(k+1) = \begin{cases} sBest(k) & if \quad f(pBest_i(k)) \leq f(sBest(k)) \\ pBest_i(k) & if \quad f(pBest_i(k)) > f(sBest(k)) \end{cases} \tag{25}$$

- Finally, a particles velocity, determining its movement in the next iteration is updated according to the following equation:

$$v_i(k+1) = \left(w \times v_i(k)\right) + (j_1 \times r_1 \times \left(pbest_i(k) - x_i(k)\right) + (j_2 \times r_2 \times (sbest(k) - x_i(k)) \quad (26)$$

The first part of the equation is known as the momentum/memory part which ensures, through the inertia constant 'w' that the new velocity of the particle does not change abruptly. The second part is known as the cognitive part in which the particle learns from its own experience. The third part is known as the social part, where the particle learns from social interactions within the swarm [48]. A large velocity increases the convergence speed along with the chances of converging towards the boundaries of the search space. However, a small value increases computation time but finds a global optimum as it increases the ability of particles to explore.

The random variables (r_1 and r_2) add a random component to the algorithm and prevent it from getting stuck at a local maxima. 'j_1' and 'j_2' are described in section 3. 'pBest' and 'sBest' are the quality factors of the algorithm ensuring diversity of particle positions [47].

- Finally, the new position of a particle is updated as:

$$x_i(k+1) = x_i(k) + v_i(k+1) \quad (27)$$

- Due to the random nature of movement, after each iteration it is necessary to check that the position of every dimension of each particle is within the search space. If not it is set equal to the closest limit. This ensures that the swarm does not explode and

follows a converging path. Once again $x_{max/min} = (x_1, x_2 \ldots . x_n)$ is a vector of 'n' dimensions.

$$If\ (x)_i > x_{max}\ then\ (x)_i = x_{max}$$
$$If\ (x)_i < x_{min}\ then\ (x)_i = x_{min} \quad (28)$$

Another important feature is the selection amongst the two neighbourhood topologies of the swarm defining the social interaction method to calculate 'sBest', of a particle [46]. The global model is known as a fully connected social network. All the particles within the swarm are interconnected to each other in terms of communication. The best position, of a particle 'pBest', is known to the entire swarm. In reality this is rarely the case, but possible in small sized swarms. The local model is known as a partial social network. Each particle is influenced only by the best performance of its neighbours which are a subset of the swarm. There are different topologies to define neighbours and compute the variable '$sBest_i$' where 'i' in this case denotes a specific neighbourhood [45]. This topology is more realistic, a bit complex and avoids convergence to a local optimum, but at a lower convergence speed.

3. Methodology and algorithms

The PSO-Neumann algorithm is simulated using MATLAB. An overview of the structure of the algorithm is in Figure 4:

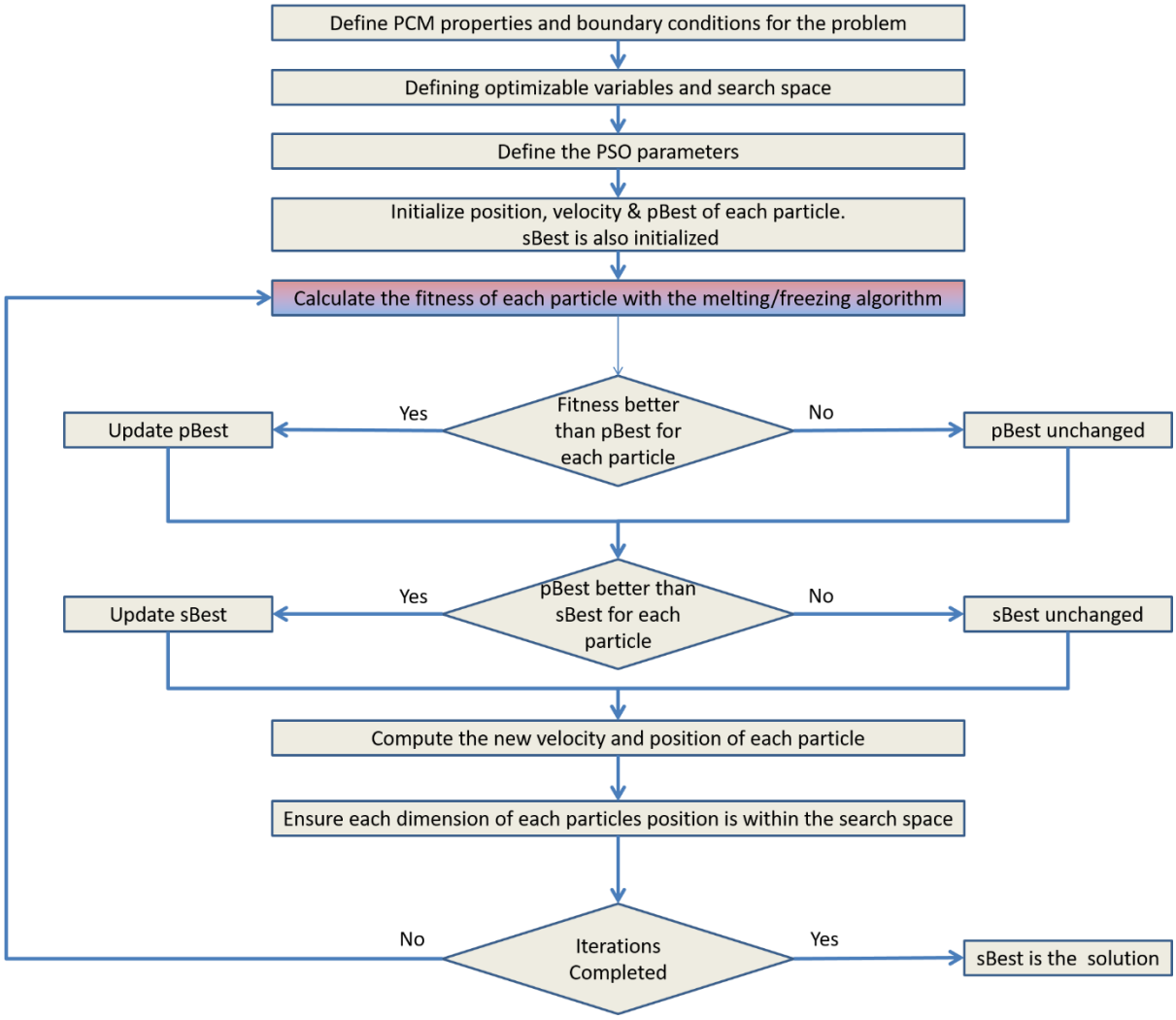

Figure 4: Overall algorithm for the melting-freezing PSO algorithm – where grey is PSO, red is melting and blue is freezing

Initially the PCM is melted to store or extract heat from the GW. After this cycle the liquid PCM is frozen to utilize this heat and insert it into the CW. The algorithm for the melting and freezing portions is as in Figure 5:

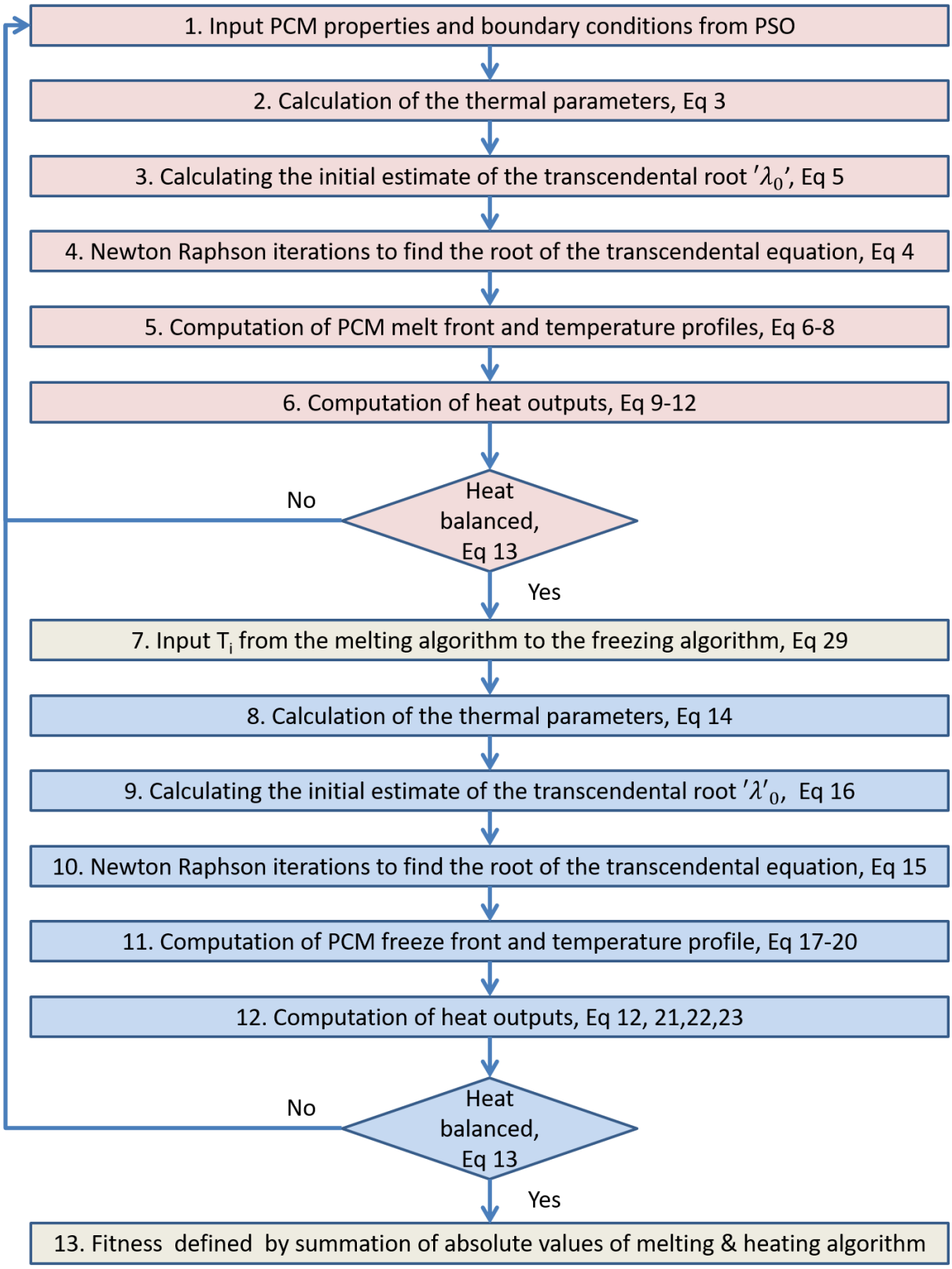

Figure 5: Melting and freezing algorithm using the Neumann solution

The Neumann solution is valid for a constant 'T_i', over the semi-infinite slab. However after the initial melting cycle, the slab has a non-uniform temperature profile. It is assumed that the initial temperature of the slab is that of the mid-point of the melt front, when passed from the melting to the freezing algorithm as of point 7 of Figure 5, using the following equation:

$$T_i^{freezing} = T_b^{melting} - (T_b^{melting} - T_m) \frac{erf\left[\frac{\left(\frac{2\lambda^{melting}\sqrt{(\alpha_L)\, t}}{2}\right)}{2\sqrt{\alpha_L t}}\right]}{erf\lambda^{melting}} \quad (29)$$

The variable 'x', in equations of the temperature profiles of the phases, represents a hypothetical point of interest from the boundary of the slab. It has no involvement in the fitness function or the outcome, but is used to visualize the temperature profile at this specific position. During the algorithm, a condition might occur outside the melt region, when '$T_i < T_m$', for this hypothetical point, when moving from the melting to freezing algorithm. In this event equation (20), calculates the temperature profile without a phase change occurrence. This algorithm takes the melt region, as the area of consideration for optimization.

As in Figure 4, the first step is to define the PCM properties and boundary conditions of the GW harnessing application. Based on the temperature profiles of the GW and CW, 'T_b' for the melting is defined as 52°C and that for freezing as 10°C. The initial temperature 'T_i', for the melting algorithm is the ambient temperature of 18°C. The PCM properties are defined based on data compiled for organic PCMs by Pluss, PureTemp, Honeywell, Rubitherm, PlusICE, SavenRG, Microtek and Croda International Plc in the range of 18-52°C. A summary of the thermal parameters from this data is in Table 2:

Table 2: Range of the thermal parameters of commercially manufactured PCMs in a T_m between 18-52°C

	Latent heat in kJ/kg	**Density in kg/m^3**	**Solid thermal conductivity in kW/(m. °C) × 10^{-3}**	**Liquid thermal conductivity in kW/(m. °C) × 10^{-3}**	**Solid specific heat capacity in kJ/(kg. °C)**	**Liquid specific heat capacity in kJ/(kg. °C)**
Max	340	2,100	0.59	32	3.51	4.19
Min	37	735	0.1	0.14	1.15	1.39
Average	187.5	1,092.5	0.2635	0.65	2.15	2.47
Standard deviation	50.5	310.2	0.185	2.84	0.35	0.62

The four variables in Table 3, are optimized through the PSO algorithm within the specified range, selected based on the differences between the average values and standard deviations of Table 2. Latent heat and specific heat capacities have been selected as optimizable variables to see whether the algorithm prefers latent or sensible heat. The thermal conductivities and density of the PCM are taken as constants, also based on average values from Table 2. The main variable of interest is 'T_m', with the range selected based on the boundary conditions of the GW application.

Table 3: Optimizable variables with the search space range for the PSO algorithm

Variable	**Interpretation**	**Range**
C_p liquid	Liquid specific heat capacity in kJ/(kg.°C)	1.9 – 3.1
C_p solid	Solid specific heat capacity in kJ/(kg.°C)	1.8-2.5
Latent heat	Latent heat for the PCM in kJ/kg	137-238
T_m	Melt temperature of the PCM in °C	18-52

Each particle has four dimensions, based on the optimizable variables, with defined search ranges in Table 3. The fitness of a particle is assessed on the absolute values of the heat

absorbed and released by the PCM during the melting (equation (9)) and freezing (equation (21)), respectively, as per the following equation:

$$f(x_i(k)) = Q_{abs} = |Q_{melt}(k)| + |Q_{freeze}(k)| \quad (30)$$

The highest value of the fitness function or maxima is desired in this application. The total time set for the simulation is 1,800 seconds. Equal times of 900 seconds are set for both the melting and freezing phases. This is based on the average time of flowing of GW, in domestic households [1].

The parameters for the PSO algorithm are defined, after several test trials on convergence to a global maxima. The number of particles in the swarm is set at 8. The optimizable variables are 4, and as mentioned the rule of thumb is to select up to a maximum of four times the number of particles based on the variables. A much larger number of particles would result in faster convergence with a chance of finding a local maxima as discussed in section 4. The number of iterations for this algorithm is set at 100. Since the search space is not vast, the solution converges quickly.

As the swarm size isn't high, the global network model is selected to update the 'sBest' variable. After tuning, the three important variables of equation (26) (w, j_1 and j_2), are assigned values of 0.6, 0.5 and 0.4 respectively. All constant variables used are summarized in Table 4:

Table 4: Input variables with fixed values

Variable	Interpretation	Value
T_b Melting	Boundary temperature i.e. GW pipe temperature for the melting algorithm in ℃	52
T_b Freezing	Boundary temperature i.e. CW pipe temperature for the freezing algorithm in ℃	10

T_i Melting	Initial temperature for the melting algorithm in ℃	18
k_L	Thermal conductivity of liquid phase in kW/(m. ℃)	0.65×10^{-3}
k_S	Thermal conductivity of solid phase in kW/(m. ℃)	0.27×10^{-3}
ρ	Phase-independent density in kg/m^3	1092.5
Time	Time for both melting and freezing, in seconds. Equal division of time between both algorithms	1800
Particles	Number of PSO particles	8
Dimensions	Number of optimizable variables defining the rows in x_i, v_i, $pBest_i$, sBest vectors of the PSO algorithm	4
Iterations	Number of iterations in the PSO algorithm	100
w	Inertia weight of the particles	0.6
j_1	Cognitive learning rate	0.5
j_2	Social learning rate	0.4

'w' is a sensitive parameter impacting the particles exploration region influencing the computation time, with a value not bigger than 1, since then the swarm would explode. A large value allows the particle to move with a large velocity, enabling it to find the optimum in a minimum amount of time. However a very large value will make the particle explore only around the edges of the search space. A small value can narrow the particles search region, to find a local optimum in a larger amount of computation time. Based on research [49], 'w' is between 0.1 to 0.9, to balance exploration and exploitation.

The movement of each particle is controlled by the acceleration constants 'j_1' and 'j_2'. Most guidelines treat the sum of the two constants[49], as the variable to be changed. The frequency of oscillations about the optimum increases proportionally to the values of these variables. For small values the trajectory of a particle is extremely long with increases in small steps. The trajectory explodes to infinity for values of their sum greater than 4.0 [49]. It is not recommended to equalize the two variables as the learning curve of a particle is rarely

equally based from both personal and social behaviour. For larger searcher domains, usually these variables are initially set at large values decaying over time.

The developed model for the Neumann solution is validated with examples from literature [38]. Similarly the validation is further proved by ensuring the energy balance of equation (13) for both melting and freezing, after every iteration. For the custom built PSO algorithm for this specific application there is no benchmark for validation. However the behaviour of the swarm is assessed over several trials to ensure no abnormalities existed. It is made certain that the entire search range is covered by plots similar to Figure 10, and the parameters are finely tuned. The outcome is intuitively assessed for its credibility and seems reasonable.

4. Results and discussion

With the defined ranges and parameters, Table 5 summarizes the optimum results obtained:

Table 5: Results of the optimum variables of the algorithm

Variable	Interpretation	Value
C_p liquid	Liquid specific heat capacity in kJ/(kg.℃)	3.1
C_p solid	Solid specific heat capacity in kJ/(kg.℃)	2.5
Latent heat	Latent heat for the PCM in kJ/kg	238
T_m	Melt temperature of the PCM in °C	20.85
Q_{abs}	Total heat absorbed and inserted in kJ	5.24155
λ_m	Root of the transcendental equation for melting	0.4147
λ_f	Root of the transcendental equation for freezing	0.1651

The first for variables correspond to the four dimensioned '$sBest$' after 100 iterations, based on the algorithm outlined in Figure 4. The first three of these variables analyse whether a sensible combination or latent combination of heat transfer is preferred. Evidently, the maximum of both is preferred as these values are at the upper limit of the range in Table 3.

The temperature profiles at the midpoint of the phase change front (5.4 mm) from the boundary, for both melting and freezing are in Figure 6:

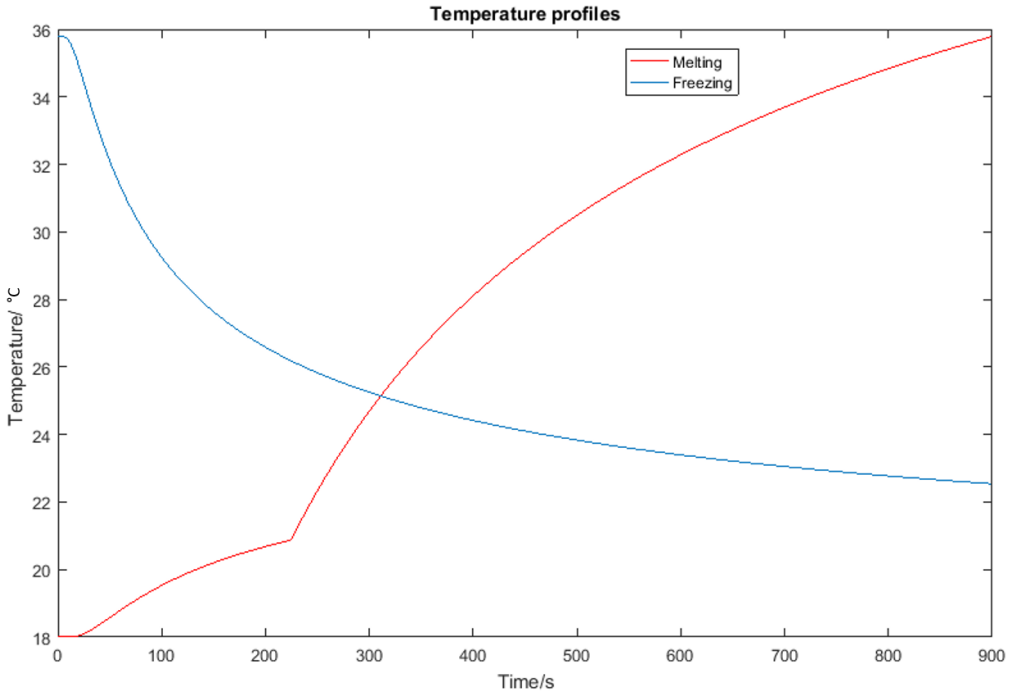

Figure 6: Temperature profiles at position x = 0.54 cm from the boundary edge of the layout

It can be seen that a prominent phase change occurs during melting at 20.85°C but not for freezing, at the position 0.54cm, probably due to the time limit of 15 minutes. However, there is freezing prior to this position as can be seen from the freeze front position of Figure 7. When the expression '$(a\lambda)^2 < 1.5$' for a PCM is true, a change in concavity occurs due to thermal property effects, as seen in the initial 100 s melt temperature profile [38]. At the same time it is also observed that both plots start from 'T_i' and asymptotically approach 'T_b', as expected.

There is no horizontal line at 'T_m' as would be expected for phase change to occur. This is a typical behaviour of the Neumann solution where the time for melt is not calculated. As soon as the melt front reaches a specific point the transition of equations takes place without

considering the melt time. In reality it is observable, with the formation of a mushy region. The propagation of the phase change fronts is presented in Figure 7:

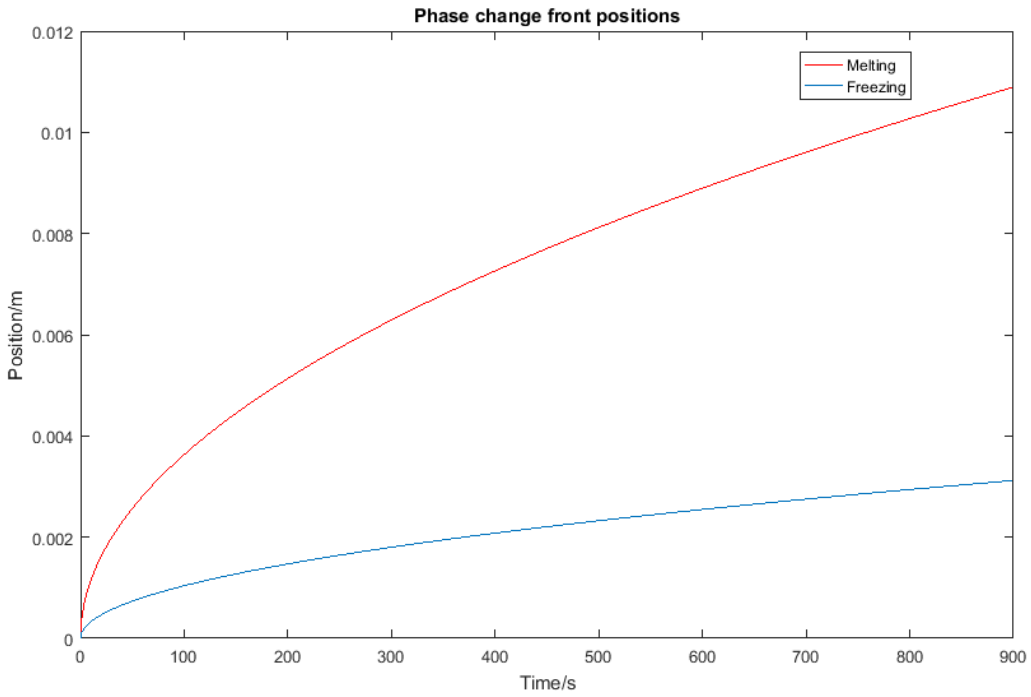

Figure 7: Propagation of phase change fronts from the boundary edge of the layout

In about 15 minutes 1.1cm of PCM, adjacent to 'T_b' is melted. In the same amount of time, only about 0.32cm of PCM adjacent to the boundary 'T_b', freezes, which is about 1/3rd compared to the melting front. Hence freezing is a much slower process primarily due to the fact that the thermal conductivity in the freezing phase is less than half of that in the liquid phase. At the same time during melting, convection effects contribute to higher heat transfer rates, although not directly considered in this model. Instead of an equal distribution of the time of 15 minutes an unequal distribution would have resulted in equal phase change front positions.

The distributions of the heat fluxes at this optimum condition for both processes are in Figure 8:

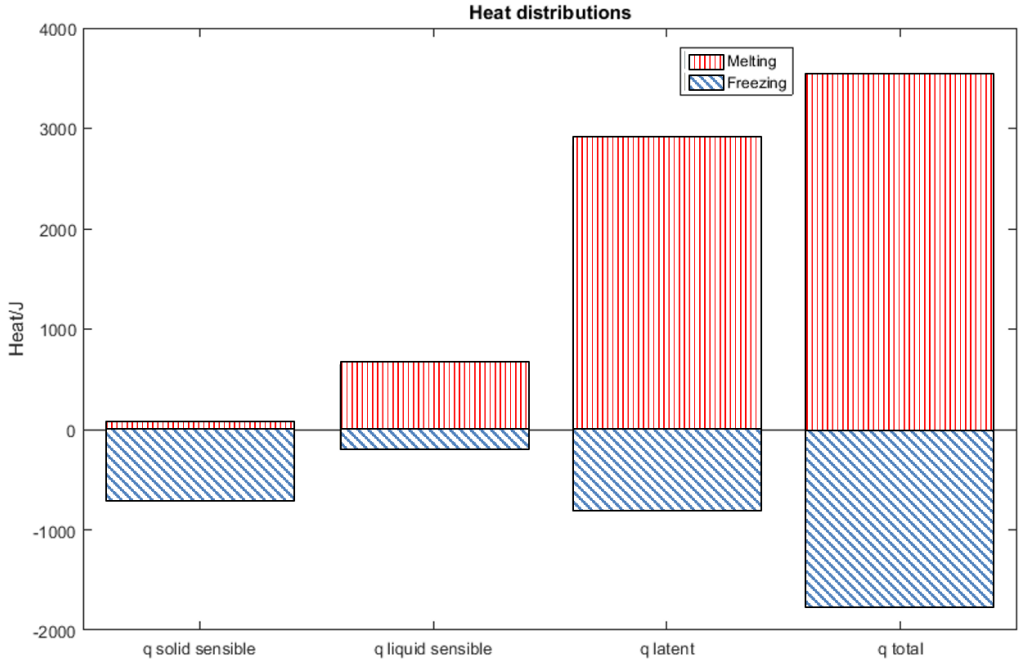

Figure 8: Heat flux distributions for the optimum fitness of the PSO

About 5.24155 kJ of total heat is transferred where 67% is contributed by melting while 33 % by freezing. This is the exact ratio of the phase change front positions of Figure 7. Latent heat is dominant in the melting process while an equal combination of latent and sensible heat contributes to the freezing process. This proves that latent heat storage has a higher storage density compared to sensible storage.

Due to the fact that the thermal parameters of sensible and latent heat are always optimum at the maximum end of the range, the solution converged quickly, as can be seen from the plot of the fitness function '$f(sBest)$' of Figure 9.

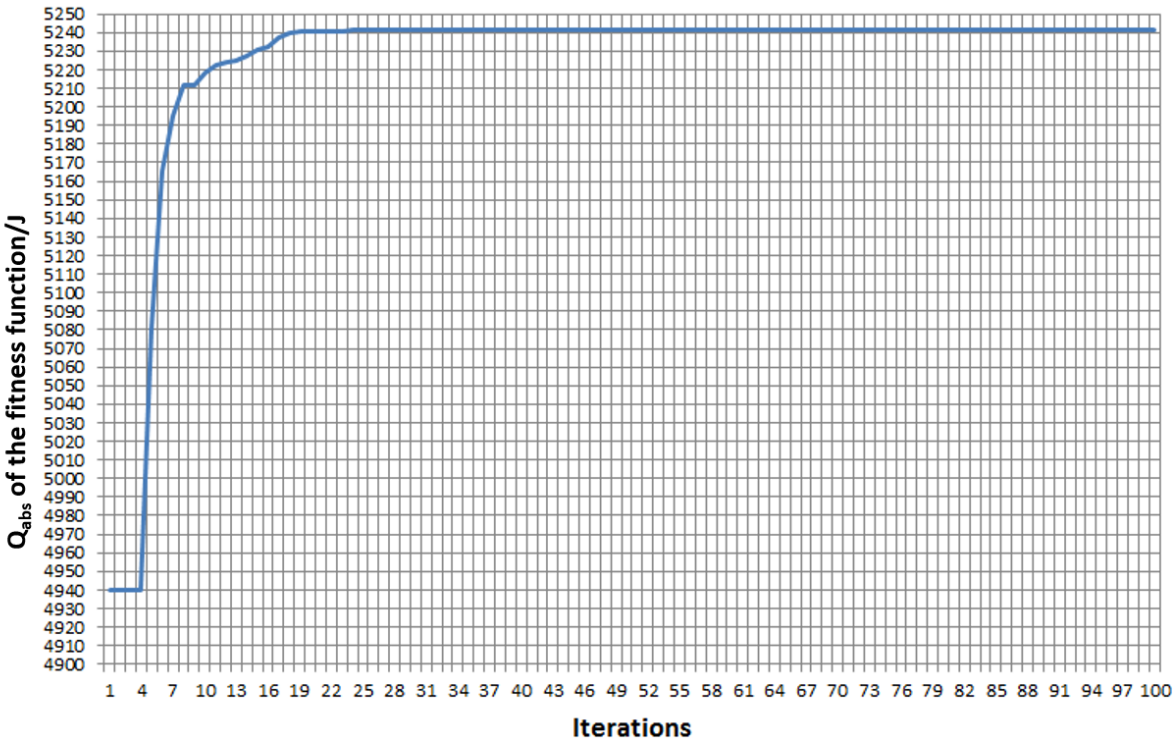

Figure 9: Convergence of the fitness function i.e. the total heat transferred

On the contrary, 'T_m' converges after more iterations. To illustrate the fact that a global maxima is actually achieved, the scatter plot of Figure 10 displays the variation of 'T_m' for each particle after every 10 iterations. Initially in iteration 1, the particles are scattered all over the search domain while finally, all of them converge to 'T_m = 20.85°C' , after the 100 iterations.

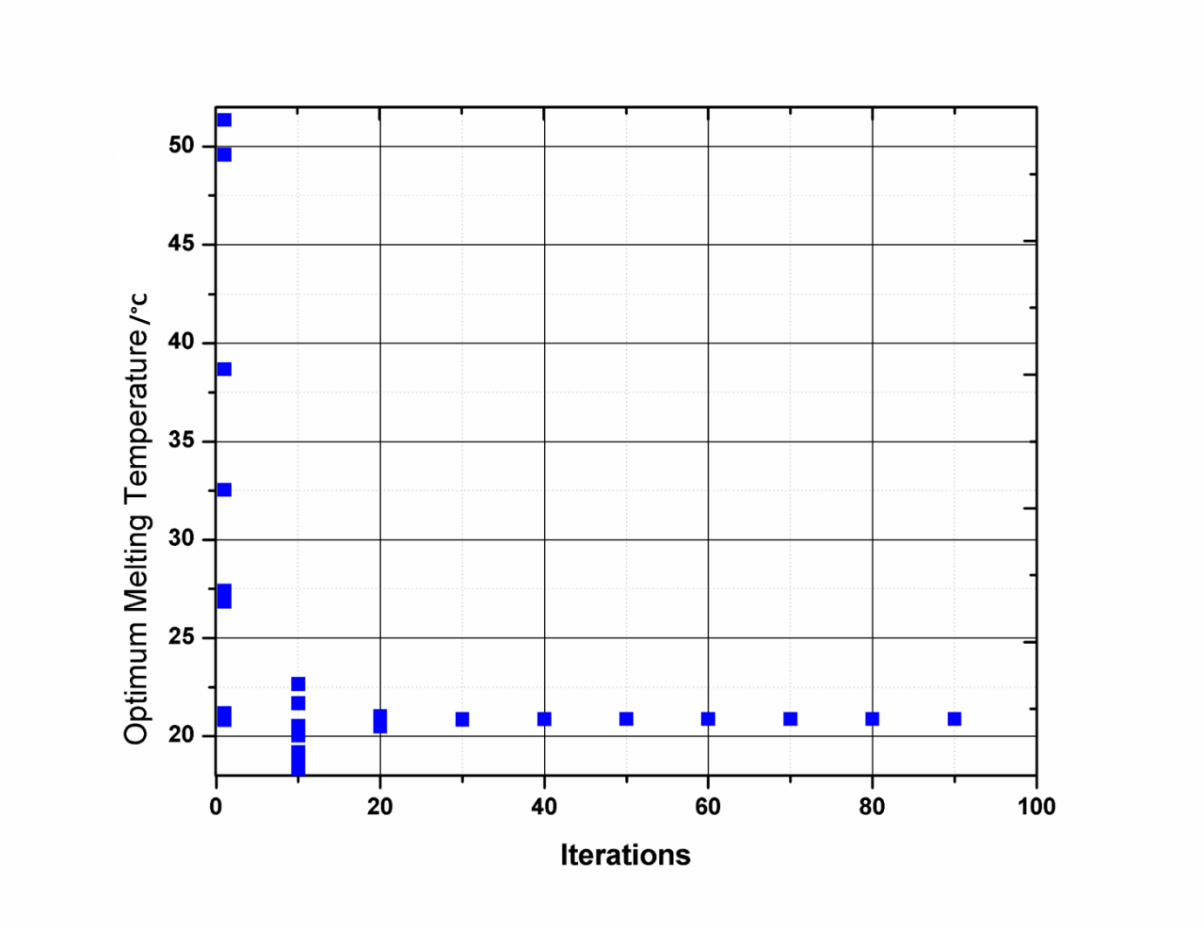

Figure 10: Convergence of optimum melt temperature

4.1. Variations in PSO parameters

The variation of the three primary variables (w, j_1 and j_2), in the PSO is performed as listed in Table 6. The complexity of using decaying variables or increasing dependency of these variables on thermal properties would have fine tuned the results further, but for this application it is kept simple.

Table 6: Parametric study of the variation of PSO parameters

Variated variable	Constant variables	Q_{abs} fitness function/kJ	T_m/°C	Maxima
w – increased to 0.90	j_1,j_2	5.24155	20.85	Global
w – decreased to 0.10	j_1,j_2	5.12734	22.59	Local
j_1 – increased to 2.0	j_1,w	5.24155	20.85	Global

j_1 – decreased to 0.1	j_1,w	5.15649	29.33	Local
j_2 – increased to 2.0	j_2,w	5.22939	18	Local
j_2 – decreased to 0.1	j_2,w	5.20285	26.49	Local

Since the search space is small in this case, most combinations except lower values of these variables converged to a global maxima. To ensure that the entire search space is thoroughly checked the number of particles could be increased resulting in faster convergence. With an increase to 20 particles and finally 50 particles, the same global maxima is reached. However if the number of particles is lowered, the probability of finding a local maxima increased. Hence the number of particles is directly proportional to the speed of convergence, upto a certain limit before saturation in the swarm. More particles result in higher computation times. Therefore a balance between the maximum particles used and computation time has to be achieved, as per application.

4.2. Variations in Neumann solution parameters

As from Table 5, the algorithm always prefers a maximum of both the sensible and latent heat variables. At the same time from Figure 8, most of the heat is input in the form of latent energy, for the melting algorithm. It can be argued that the upper limit is a bit out of range, for most practical combinations. Hence the upper limits of the three variables 'c_p liquid', 'c_p solid' and 'L latent heat' are decreased. The upper limits for 'c_p liquid' and 'c_p solid' are changed to 2.2 kJ/(kg.°C) and 2.0 kJ/(kg.°C) respectively. The input of the the upper limit of the latent heat is varied, giving a linear relationship with 'T_m', as in Figure 11:

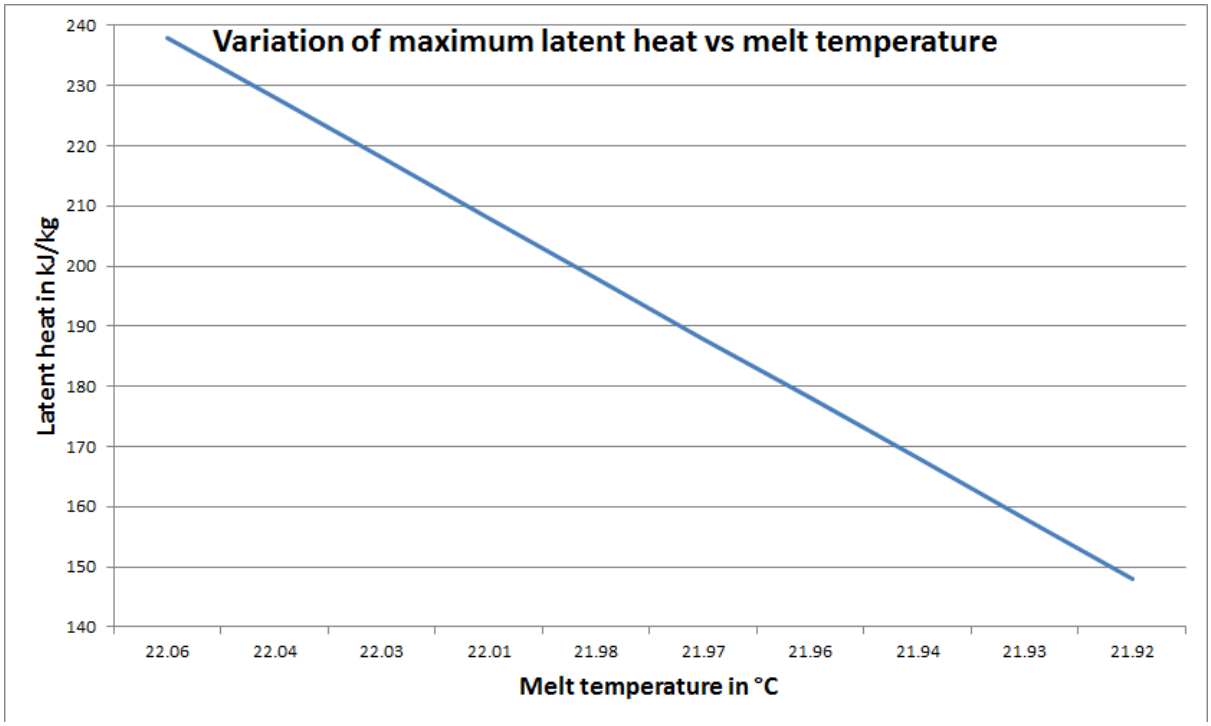

Figure 11: Variation of input maximum latent heat and optimized melt temperature

As expected the optimizer always selects a combination with the maxima heat trasnfer. Most of the heat is added in the melting phase, with the majority being latent. When the 'ΔT' between the 'T_b' and 'T_m' is greatest more latent heat via melting can be added. To compensate for the loss of latent heat energy, there is a decrease in 'T_m', to increase heat trasnfer.

It is also arguable that the time of GW flow has a normal distribution from the mean 15 minutes [1]. Hence a variation of time is also investigated from the initially set 15 minutes. However the results are independent of time. Probably an unequal distribution, with a higher time for freezing would have invoked different results.

5. Conclusion

An optimizer using the PSO algorithm to determine the thermal parameters of a PCM has been developed, which has been applied with the GW heat harnessing. This methodology can be used in the primary phase of the design process, without the need of extensive detail.

- The Neumann solution of the Stefan problem is a good estimation of selecting a PCM for both a melting and freezing phenomena, without the practical constraints of dimensioning and analysing external factors.
- The thermal parameters are selected based on the PSO optimization algorithm linked with the Neumann solution for both melting and freezing. The PSO procedure is suitable for this multi-variable non-linear problem with convergence to the desired maxima of heat extracted/inserted.
- Results show that the best performance PCM for this application would have a 'T_m' of 20.85°C. However a sensitivity analysis of parameters from both the PSO and Neumann solution provide an insight into the complexities. It can be seen that melting is relatively a faster phenomenon, compared to freezing.

The basic Neumann solution can easily be replaced with more detailed implicit approximations, within this algorithm for further studies. At the same time detailed numerical and experimental analysis of this optimum PCM is recommended after this selection phase.

Abbreviations

PCM	Phase change material
PSO	Particle swarm optimization
GW	Grey water
CW	Cold water
CFD	Computational fluid dynamics

L and S subscripts	Liquid and solid region
Sens	Sensible Heat
Lat	Latent heat

Nomenclature

T_m	Melting temperature in °C
∇	Laplace operator
T	Temperature in °C
t	Time in seconds
α	Thermal diffusivity in m^2/s
$\dot{q}$/q	Internal heat generation rate in W
T_i	Initial temperature in °C
T_b	Boundary temperature in °C
L	Latent heat kJ/kg
v	Velocity in m/s
ρ	Density in kg/m^3
$X(t)$	Position of the melt front in m
k	Thermal conductivity of liquid phase kW/(m.°C)
x	Position in m
∞	Infinity
St	Stefan number
c	Specific heat in kJ/(kg.°C)
a	Ratio of the under root of the thermal diffusivities
λ	Root of the transcendental equation
exp	Exponential
erf	Error function
erfc	Complementary error function
π	Pi
Q	Heat energy in kJ
n	Number of dimensions in the PSO
x_i	Position vector of the PSO
v_i	Velocity vector of the PSO
k	Iteration number
$f(x)$	Fitness function for the PSO
$pBest_i$	Particle best vector of the PSO
sBest	Swarm best vector of the PSO
w	Inertia weight of the particle
j_1	Cognitive learning rate
r	Random variable between 0 -1
j_2	Social learning rate
Δ	Delta or change

References

[1] Mazhar AR, Liu S, Shukla A. A Key Review of Non-Industrial Greywater Heat Harnessing. Energies 2018;11. doi:10.3390/en11020386.
[2] Chiong R. Nature-Inspired Algorithms for Optimisation. Warsaw: Springer; 2009.
[3] Gu Z, Liu H, Li Y. Thermal energy recovery of air conditioning system - Heat recovery system calculation and phase change materials development. Appl Therm Eng 2004;24:2511–26. doi:10.1016/j.applthermaleng.2004.03.017.
[4] Mousa H, Gujarathi AM. Modeling and analysis the productivity of solar desalination units with phase change materials. Renew Energy 2016;95:225–32. doi:10.1016/j.renene.2016.04.013.
[5] López-Sabirón AM, Royo P, Ferreira VJ, Aranda-Usón A, Ferreira G. Carbon footprint of a thermal energy storage system using phase change materials for industrial energy recovery to reduce the fossil fuel consumption. Appl Energy 2014;135:616–24. doi:10.1016/j.apenergy.2014.08.038.
[6] Nomura T, Okinaka N, Akiyama T. Waste heat transportation system, using phase change material (PCM) from steelworks to chemical plant. Resour Conserv Recycl 2010;54:1000–6. doi:10.1016/j.resconrec.2010.02.007.
[7] Zhao J, Ji Y, Yuan Y, Zhang Z, Lu J. Energy-Saving Analysis of Solar Heating System with PCM Storage Tank. Energies 2018;11. doi:10.3390/en11010237.
[8] Ihm P, Krarti M, Henze GP. Development of a thermal energy storage model for EnergyPlus. Energy Build 2004;36:807–14. doi:10.1016/j.enbuild.2004.01.021.
[9] Asbik M, Ansari O, Bah A, Zari N, Mimet A, El-ghetany H. Exergy analysis of solar desalination still combined with heat storage system using phase change material (PCM). DES 2016;381:26–37. doi:10.1016/j.desal.2015.11.031.
[10] Klein Altstedde M, Rinderknecht F, Friedrich H. Integrating phase-change materials into automotive thermoelectric generators: An experimental examination and analysis of energetic potential through numerical simulation. J Electron Mater 2014;43:2134–40. doi:10.1007/s11664-014-2990-z.
[11] Shon J, Kim H, Lee K. Improved heat storage rate for an automobile coolant waste heat recovery system using phase-change material in a fin-tube heat exchanger. Appl Energy 2014;113:680–9. doi:10.1016/j.apenergy.2013.07.049.
[12] Fadaei N, Kasaeian A, Akbarzadeh A. Experimental investigation of solar chimney with phase change material (PCM). Renew Energy 2018;123:26–35. doi:10.1016/j.renene.2018.01.122.
[13] Ar M, Bilgin F, Ni S. Phase change material based cooling of photovoltaic panel : A simplified numerical model for the optimization of the phase change material layer and general economic evaluation. J Clean Prod 2018;189:738–45. doi:10.1016/j.jclepro.2018.04.057.
[14] Zhao R, Gu J, Liu J. Optimization of a phase change material based internal cooling system for cylindrical Li-ion battery pack and a hybrid cooling design. Energy 2017;135:811–22. doi:10.1016/j.energy.2017.06.168.
[15] Zwanzig SD, Lian Y, Brehob EG. Numerical simulation of phase change material composite wallboard in a multi-layered building envelope. Energy Convers Manag 2013;69:27–40. doi:10.1016/j.enconman.2013.02.003.
[16] Annulus H, Li S, Chen Y, Sun Z. Numerical Simulation and Optimization of the Melting Process of Phase Change Material inside Horizontal Annulus. Energies 2017;10. doi:10.3390/en10091249.
[17] Virgone J, Noel J. Optimization of a phase change material wallboard for building use. Appl Therm Eng 2008;28:1291–8. doi:10.1016/j.applthermaleng.2007.10.012.
[18] Prabu SS, Asokan MA. A study of waste heat recovery from diesel engine exhaust using phase change material. Int J ChemTech Res 2015;8:711–7.
[19] Salyan S, Suresh S. Liquid metal gallium laden organic phase change material for energy storage : An experimental study. Int J Hydrogen Energy 2017;43:2469–83. doi:10.1016/j.ijhydene.2017.12.047.
[20] Zhang X, Yu S, Yu M, Lin Y. Experimental research on condensing heat recovery using phase change material. Appl Therm Eng 2011;31:3736–40. doi:10.1016/j.applthermaleng.2011.03.040.
[21] Nagano K, Ogawa K, Mochida T, Hayashi K, Ogoshi H. Thermal characteristics of magnesium nitrate hexahydrate and magnesium chloride hexahydrate mixture as a phase change material for effective utilization of urban waste heat. Appl Therm Eng 2004;24:221–32. doi:10.1016/j.applthermaleng.2003.09.003.
[22] Li W, Li S, Guan S, Wang Y, Zhang X. Numerical study on melt fraction during melting of phase change material inside a sphere. Int J Hydrogen Energy 2017;42:18232–9. doi:10.1016/j.ijhydene.2017.04.136.
[23] Park S, Woo S, Shon J, Lee K. Numerical model and simulation of a vehicular heat storage system with phase-change material. Appl Therm Eng 2017;113:1496–504. doi:10.1016/j.applthermaleng.2016.11.162.
[24] Bhagat K, Saha SK. Numerical analysis of latent heat thermal energy storage using encapsulated phase change material for solar thermal power plant. Renew Energy 2016;95:323–36.

doi:10.1016/j.renene.2016.04.018.
[25] Joulin A, Younsi Z, Zalewski L, Lassue S, Rousse DR, Cavrot J. Experimental and numerical investigation of a phase change material : Thermal-energy storage and release. Appl Energy 2011;88:2454–62. doi:10.1016/j.apenergy.2011.01.036.
[26] Lamberg P, Lehtiniemi R, Henell A. Numerical and experimental investigation of melting and freezing processes in phase change material storage. Int J Therm Sci 2004;43:277–87. doi:10.1016/j.ijthermalsci.2003.07.001.
[27] Dadollahi M, Mehrpooya M. Modeling and investigation of high temperature phase change materials (PCM) in different storage tank configurations. J Clean Prod 2017;161:831–9. doi:10.1016/j.jclepro.2017.05.171.
[28] Gracia A De, Oró E, Farid MM, Cabeza LF. Thermal analysis of including phase change material in a domestic hot water cylinder. Appl Therm Eng 2011;31:3938–45. doi:10.1016/j.applthermaleng.2011.07.043.
[29] Mawire A, Abedigamba OP, Beemkumar N, Karthikeyan A. Charging and Discharging Processes of Thermal Energy Storage System Using Phase change materials. IOP Conf Ser Mater Sci Eng 2017. doi:10.1088/1757-899X/197/1/012040.
[30] Thomas J, Srivatsa PVSS, S RK, Baby R. Thermal Performance Evaluation of a Phase Change Material Based Heat Sink : A Numerical Study. Procedia Technol 2016;25:1182–90. doi:10.1016/j.protcy.2016.08.237.
[31] Mamode M. Two Phase Stefan problem with boundary temperature conditions: An analytical approach. SIAM J Appl Math 2013;73:460–74. doi:10.1137/110852474.
[32] Sharma A, Tyagi V V., Chen CR, Buddhi D. Review on thermal energy storage with phase change materials and applications. Renew Sustain Energy Rev 2009;13:318–45. doi:10.1016/j.rser.2007.10.005.
[33] Dubovsky V, Ziskind G, Letan R. An Analytical Technique of Transient Phase- Change Material Melting Calculation for Cylindrical and Tubular Containers. Heat Transf Eng 2018;0:1–14. doi:10.1080/01457632.2018.1457271.
[34] Mosaffa A, Talati F, Rosen MA, Basirat TH. Phase change material solidification in a finned cylindrical shell thermal energy storage: An approximate analytical approach. Therm Sci 2013;17:407–18. doi:10.2298/TSCI120326207M.
[35] Dutil Y, Rousse DR, Salah N Ben, Lassue S, Zalewski L. A review on phase-change materials: Mathematical modeling and simulations. Renew Sustain Energy Rev 2011;15:112–30. doi:10.1016/j.rser.2010.06.011.
[36] Zhaochun W, Jianping L, Jingmei F. A novel algorithm for solving the classical Stefan problem. Therm Sci 2011;15:39–44. doi:10.2298/TSCI11S1039W.
[37] Salvatori L, Tosi N. Stefan problem through extended finite elements: Review and further investigations. Algorithms 2009;2:1177–220. doi:10.3390/a2031177.
[38] Alexiades V, Solomon AD. Mathematical Modeling of Melting and Freezing Processes. Washington: Taylor & Francis; 1993.
[39] Carslaw H., Jaeger J. Conduction of Heat in Solids. Second. London: Oxford University Press; 1959.
[40] Fleischer AS. Thermal Energy Storage Using Phase Change Materials Fundamentals and Applications. SpringerBr. Minneapolis: Springer; 2015. doi:10.1007/97-3-319-20922-7.
[41] Rubinstein L. The Stefan Problem. Volume 27. American Mathematical Society; 1971.
[42] Manzano-agugliaro F, Montoya FG, Gil C, Alcayde A, Gómez J, Ba R. Optimization methods applied to renewable and sustainable energy : A review. Renew Sustianable Energy Rev 2011;15:1753–66. doi:10.1016/j.rser.2010.12.008.
[43] Selvi V, Umarani R. Comparative Analysis of Ant Colony and Particle Swarm Optimization Techniques. Int J Comput Appl 2010;5:1–6.
[44] Pal SK, Rai C., Singh AP. Comparative Study of Firefly Algorithm and Particle Swarm Optimization for Noisy Non-Linear Optimization Problems. Int J Intell Syst Appl 2012;4:50–7. doi:10.5815/ijisa.2012.10.06.
[45] Yang B. Modified Particle Swarm Optimizers and their Application to Robust Design and Structural Optimization. Technische Universität München, 2009.
[46] Eberhart R, Kennedy J. A New Optimizer Using Particle Swarm Theory. IEEE 6th Int Symp Micro Mach Hum Sci 1995:39–43.
[47] AlRashidi M., El-Hawary M. A Survey of Particle Swarm Optimization Applications in Electric Power Systems. IEEE Trans EEolutionary Comput 2009;13:913–8. doi:10.1109/TEVC.2006.880326.
[48] Sharaf AM, El-gammal AAA. Computational Intelligence in Power Engineering. Heidelberg: Springer; 2010.
[49] Eberhart C, Shi Y. Comparing inertia weights and constriction factors in particle swarm optimization. Proc 2000 Congr Evol Comput 2000:84–8. doi:10.1109/CEC.2000.870711.